

Multi-valued versus single-valued large-amplitude bending-torsional-rotational coordinate systems for simultaneously treating trans-bent and cis-bent acetylene in its S_1 state

Jon T. Hougen*

Sensor Science Division, National Institute of Standards and Technology, Gaithersburg, MD 20899-8441, USA

ARTICLE INFO

Article history:

Received 30 May 2012

In revised form 13 July 2012

Available online 28 July 2012

Keywords:

Acetylene

Boundary conditions

Extended permutation-inversion groups

Large amplitude motions

Multiple-valued coordinate systems

S_1 state

Trans bent and cis bent forms

ABSTRACT

There are now a large number of papers in the spectroscopic literature which make use of multiple-valued (frequently double-valued) coordinate systems and the associated multiple-groups of the permutation-inversion group to deal with the symmetry properties of large-amplitude motions in molecules of high symmetry. The use of multiple-valued coordinate systems, and the resultant appearance of more minima on the potential surface than would be found on the surface for a single-valued coordinate system, can lead to conceptual confusion and questions of mathematical legitimacy. In the present paper we demonstrate that treatments using multiple-valued coordinate systems simply represent one scheme for applying the appropriate quantum mechanical boundary conditions to Schrödinger's partial differential equation defined in a single-valued coordinate system. The demonstration is not general, but rather focuses on the specific example of the S_1 electronic state of C_2H_2 , which has local minima only for non-linear configurations, and on the twofold and eightfold extended permutation-inversion groups recently introduced to simultaneously treat symmetry questions in trans-bent and cis-bent acetylene. Some discussion of the mathematical convenience lost by using a single-valued coordinate system is also presented.

© 2012 Elsevier Inc. All rights reserved.

1. Introduction

Recently, a simultaneous group theoretical treatment of trans-bent and cis-bent acetylene in the first excited singlet electronic state S_1 has been presented [1], which assumed no C–H bond breaking and was based on a permutation-inversion (PI) group of order 4, but which also made use of multiple-valued molecule-fixed coordinate systems and their corresponding extended PI groups. A similar treatment of trans-bent acetylene, cis-bent acetylene, and vinylidene was also given [1], but for this case, C–H bond breaking must be allowed and the PI group is of order 8. The purpose of the present paper is to show that treatments using multiple-valued coordinate systems represent an alternative way of imposing the proper quantum mechanical boundary conditions on solutions of Schrödinger's equation in a single-valued coordinate system. In particular, simple two and three-dimensional shapes (i.e., portions of squares and cubes) are used to visualize the different ranges allowed for coordinates in a multiple-valued versus a single-valued treatment, as well as to visualize the increase in complexity of the boundary conditions and of the symmetry-induced coordinate transformations that must be applied to quantum mechanically

allowed wavefunctions in single-valued coordinate treatments. To prevent extensive repetition of material already in the literature, references to equations and tables in [1] indicate where omitted mathematical details on the multiple-valued coordinate treatments can be found. To avoid complications associated with quasi-linear molecules, where the instantaneous A rotational constant becomes infinite when the large-amplitude bending motion passes through the linear configuration, we assume that all molecular eigenstates under consideration here are well below the energy of the high barrier to linearity in the S_1 state shown in Fig. 3a of [2], so that the $|\Psi|^2$ wavefunction density at the linear configuration can be taken to be zero, both when solving Schrödinger's equation and when calculating all physical observables.

This paper is divided into two parts. In Sections 2–5 we consider only two large-amplitude motions (LAMs) to be feasible in non-linear $H_1-C_a-C_b-H_2$, namely the local $H_1-C_a-C_b$ and $C_a-C_b-H_2$ bends at the two ends of the molecule. In Sections 6–8 we consider internal rotation about the C_a-C_b bond of the trans or cis bent molecule to also be feasible, leading to a total of three LAMs. We do not treat in this paper the acetylene \leftrightarrow vinylidene case [1], where breaking of the H_1-C_a and C_b-H_2 bonds must be considered.

Although some economy of presentation can be achieved by first treating the three-LAM bending-torsional problem, and then specializing to the two-LAM bending problem, the opposite order

* Fax: +1 301 869 5700.

E-mail address: jon.hougen@nist.gov

of presentation (i.e., from the simpler situation to the more complicated) is pedagogically preferable. In fact, the main ideas are all illustrated by the two-LAM discussion, which has the added advantage that concrete examples of wavefunctions for this case, computed by Baraban et al. [3] using a double-valued coordinate system, are already available in the literature. Readers not interested in the additional complications of a three-LAM treatment of bent acetylene can skip Sections 6–8 and go directly to the discussion in Section 9.

2. Some possible coordinate systems when only two bending LAMs are feasible

The most obvious single-valued coordinate system for the present problem is just the set of Cartesian coordinates in the laboratory of the four acetylene atoms. However, even after removing the center of mass, this still leaves a nine-dimensional computational problem, in which the coordinates are not closely related to the structural and chemical bonding concepts that most spectroscopists are interested in.

We therefore choose, from among the relatively large number of molecule-fixed coordinate systems that can be devised for this two-LAM problem in C_2H_2 , to work with coordinates that are closely related to the ideas of overall rotation and small-amplitude vibrations about an instantaneous chemical structure. In order to avoid the necessity of redoing large amounts of algebra to make the comparisons desired here, we follow the coordinate definitions and other notation used in Section 6 of Ref. [1]. In particular, we relate the laboratory-fixed coordinates \mathbf{R}_i of each acetylene atom $i = a, b, 1$, and 2 to various molecule-fixed coordinates via the equation

$$\mathbf{R}_i = \mathbf{R} + S^{-1}(\chi, \theta, \phi)[\mathbf{a}_i(\beta_1, \beta_2) + \mathbf{d}_i]. \quad (1)$$

In moving between single-valued and multiple-valued coordinate systems in the discussion below we will not change the definitions of the LAMs, nor will we change the form of Eq. (1). Instead we will simply change the numerical ranges allowed for the various coordinates.

Eq. (1) has the following properties of importance for the present problem. (i) Neither the location of the center of mass in the laboratory \mathbf{R} , nor the infinitesimal vibrational displacements \mathbf{d}_i on the right side of this equation are of interest, so for simplicity, we set $\mathbf{R} = \mathbf{0}$ and $\mathbf{d}_i = \mathbf{0}$ for the remainder of this paper. (ii) Traditional rotational (Eulerian) angles χ, θ, ϕ are used to relate the molecule-fixed x, y, z axes to the laboratory-fixed X, Y, Z axes via the direction cosine matrix in Eq. (2) of [1]. This implies that we expect overall rotational motion in acetylene to resemble that of a body characterized by “an approximately constant” moment-of-inertia tensor. Such an assumption is not too far from reality, since the values of the B and C rotational constants in the present problem are mainly determined by the carbon mass and the C–C equilibrium bond distance, while the value of the A rotational constant is mainly determined by the C–H equilibrium bond length and the approximately 120° C–C–H bond angles of either trans-bent or cis-bent acetylene. Even at the half-linear transition state [2,4] between the trans and cis structures (a configuration in which the molecule spends little time, at least at lower energies), the A value is only doubled. (iii) Only two LAMs, β_1 and β_2 , are introduced, which represent, respectively, the $H_1-C_a-C_b$ and $C_a-C_b-H_2$ local bending angles, as illustrated in Fig. 3a of [1].

2.1. Coordinate ranges and symmetry transformations used in Ref. [1] for Fig. 1a

Fig. 1a illustrates, in the form of a square, the ranges of the LAM coordinates β_1 and β_2 used for the double-valued coordinate

treatment in Ref. [1], to which the reader is referred for many details not repeated here. For brevity we write $\beta_1, \beta_2 \in [-2\pi/3, +2\pi/3]$. The ranges of the rotational coordinates are not shown graphically, but as usual, $\chi, \phi \in [0, 2\pi]$ and $\theta \in [0, \pi]$.

As discussed in [1], these molecule-fixed coordinates are double-valued for the following reason. If we define a given laboratory-fixed configuration to mean that each of the four labeled acetylene atoms has its own specified location in the laboratory, then two different combinations of the molecule-fixed coordinates correspond to exactly the same laboratory-fixed configuration. The two different combinations for a given laboratory configuration can be represented in row vector notation as $[\beta_1, \beta_2, \chi, \theta, \phi] = [\beta_1^\circ, \beta_2^\circ, \chi^\circ, \theta^\circ, \phi^\circ]$ or $[-\beta_1^\circ, -\beta_2^\circ, \chi^\circ + \pi, \theta^\circ, \phi^\circ]$, where symbols with a superscript $^\circ$ represent fixed numerical values. Note that both of these row vectors have the same values for the rotational angles θ and ϕ , i.e., they both have their z axis pointing in the same direction in the laboratory.

The symmetry transformations applied to functions of these coordinates [5] and the character table of the resulting extended PI symmetry group $G_4^{(2)}$ are given in Tables 5 and 6 of [1]. The group $G_4^{(2)}$ is a double group of the acetylene PI group G_4 , where G_4 contains the operations $E, (ab)(12), (ab)(12)^*$ and E^* . When bond-breaking is considered to be infeasible (as here), neither (ab) nor (12) can occur by itself in the PI group.

The dot-filled circle centered at the origin in Fig. 1a indicates the area forbidden to the molecular wavefunction because of the high barrier to linearity [2]. The three concentric circles in the upper left and lower right of Fig. 1a schematically indicate the two trans wells [2] in this double-valued coordinate system. The two concentric circles in the lower left and upper right indicate the shallower cis wells [2].

2.2. Coordinate ranges and symmetry transformations for use with Fig. 1b

Consider now the first of three single-valued coordinate systems defined by restricting the allowed range of the bending angles. If internal rotation is not allowed, then it is impossible to go from the trans to the cis configuration if β_1 and β_2 are both constrained to be positive (as one might wish to do by analogy with the bending angle of a linear molecule, for example). It is possible, however, to keep one of these two angles positive at all times. Fig. 1b illustrates this case, in the form of a rectangle covering the upper half of the square in Fig. 1a, and therefore containing only one trans and only one cis minimum. The ranges of the LAM coordinates β_1 and β_2 for this choice of a single-valued molecular coordinate system are $\beta_1 \in [0, +2\pi/3]$ and $\beta_2 \in [-2\pi/3, +2\pi/3]$. The ranges of the rotational coordinates remain unchanged, i.e., $\chi, \phi \in [0, 2\pi]$, and $\theta \in [0, \pi]$. Since there were originally two points within the square of Fig. 1a corresponding to exactly the same laboratory configuration, it is reasonable to expect that a rectangle half the size of the square would eliminate the redundancy in the molecule-fixed coordinates. This can be verified by noting that if the first set of coordinates with superscript $^\circ$ in the previous section lies within the upper rectangle, then the second set lies below that rectangle.

Coordinate transformations that are permissible for the rectangle in Fig. 1b can be selected from those given in Table 5 of [1] by noting that transformations permitted here cannot make β_1 negative, and also cannot exchange β_1 and β_2 because of the different ranges for these two variables. The PI group thus contains only the elements labeled $E = E$ and $E^* = \sigma(xz)$ in the PI and PG columns, respectively, of Table 5 of [1], where

$$\begin{aligned} \sigma(xz)\Psi(\beta_1, \beta_2, \chi, \theta, \phi) &= E^*\Psi(\beta_1, \beta_2, \chi, \theta, \phi) \\ &= \Psi(\beta_1, \beta_2, \pi - \chi, \pi - \theta, \pi + \phi). \end{aligned} \quad (2)$$

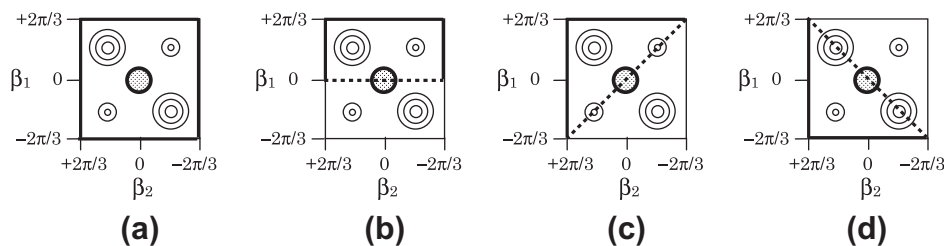


Fig. 1. Schematic potential energy surface for the S_1 state of acetylene plotted as contour lines in the β_1, β_2 bending vibrational space (after Fig. 3a of [2] and Fig. 1 of [3], but using the bending angle notation of Fig. 4 of [1]). The rotational variables have their usual ranges, $\chi, \phi \in [0, 2\pi]$ and $\theta \in [0, \pi]$. (a) The ranges shown here for the LAM bending coordinates, $-2\pi/3 \leq \beta_1, \beta_2 \leq +2\pi/3$, are those used in [1]. This coordinate domain is double-valued and contains two trans wells (shown as deeper, by three concentric circles) and two cis wells (shown as shallower by two concentric circles), as well as a high barrier at the linear configuration (shown as a dot-filled circle centered at the origin). Boundary conditions require that $\Psi \rightarrow 0$ on the heavy solid lines forming the edges of the square and the circumference of the small dot-filled circle. (b) A rectangular domain, with ranges $0 \leq \beta_1 \leq 2\pi/3$ and $-2\pi/3 \leq \beta_2 \leq +2\pi/3$ for the bending coordinates, that contains only one trans and one cis well and gives a single-valued coordinate system. The coordinate ranges for this domain do not permit exchanging the two local mode bending coordinates (see text). Boundary conditions require that $\Psi \rightarrow 0$ on the heavy solid lines where the potential energy $V(\beta_1, \beta_2) \rightarrow \infty$, but must be determined by other considerations on the heavy dashed line, where V is mostly finite. (c) A triangular domain $-2\pi/3 \leq \beta_1 \leq +2\pi/3$ and $-\beta_1 \leq \beta_2 \leq +2\pi/3$ for the bending coordinates that contains one trans and one cis well and gives a single-valued coordinate system. These coordinate ranges permit exchanging the two local mode bending coordinates via the $\beta_1 \leftrightarrow \beta_2$ symmetry operation. Boundary conditions require that $\Psi \rightarrow 0$ on the heavy solid lines, but not on the heavy dashed diagonal line, where V is mostly finite. (d) An alternative triangular domain $-2\pi/3 \leq \beta_1 \leq +2\pi/3$ and $+\beta_1 \leq \beta_2 \leq +2\pi/3$ for the bending coordinates with properties similar to Fig. 1c, except that the long side of this triangle cuts through the trans wells rather than through the cis wells, and the two local mode bends are exchanged via $\beta_1 \leftrightarrow -\beta_2$.

The resulting PI group, containing E and E^* , has only two symmetry species, which we can call A' and A'' .

The lack of the important $\beta_1 \leftrightarrow \beta_2$ symmetry operation, and the associated absence of the PI operations $(ab)(12)$ and $(ab)(12)^*$ in the operations chosen from Table 5 of [1], is a deficiency of this coordinate system which will ultimately cause us to abandon it. Before doing so, however, we note that it must somehow be possible, almost no matter what coordinate system is used, to change variables in such a way that the final result is, for example, the exchange of identical particles represented by $(ab)(12)$. Table 5 of [1] indicates that the permutation $(ab)(12)$ can be carried out in the coordinate system of this section if we use the operation $(ab)(12) = C_2(y)$ when $\beta_2 \geq 0$, and the operation $(ab)(12) = C_2(y)E_b$ when $\beta_2 < 0$, where E_b is the limited identity of the double group $G_4^{(2)}$ [1]. These two operations can be formally unified by defining a sign factor $s \equiv \beta_2/|\beta_2| = \pm 1$, and then defining the action of $(ab)(12)$ on a wavefunction as

$$(ab)(12)\Psi(\beta_1, \beta_2, \chi, \theta, \phi) = \Psi(s\beta_2, s\beta_1, (1+s)\pi/2 - \chi, \pi - \theta, \pi + \phi). \quad (3)$$

In particular, Eq. (3) shows that β_1 (which can only be positive) must be replaced by the absolute value of β_2 (which can take both positive and negative values), since $s\beta_2 = (\beta_2/|\beta_2|)\beta_2 = |\beta_2|$. We further note that $\beta_1 \rightarrow |\beta_2|$ is not a linear transformation (because of the absolute value sign), whereas the whole formalism obtained by mapping symmetry operations onto group elements in quantum mechanics is based on the assumption that the symmetry operations correspond to linear transformations of variables. Thus, even though we can define a symmetry operation $(ab)(12)$ in the coordinate system of this section, it is a nonlinear operator, and we cannot use the formalism of traditional group theory to derive conclusions from this symmetry operation.

2.3. Coordinate ranges and symmetry group for use with Fig. 1c

In an effort to find a single-valued coordinate range which permits the $\beta_1 \leftrightarrow \beta_2$ exchange, we are led to consider the upper left triangular half of the square in Fig. 1a, as shown in Fig. 1c. The LAM coordinate ranges for this triangle can then be expressed either as $\beta_1 \in [-2\pi/3, +2\pi/3]$, $\beta_2 \in [-\beta_1, +2\pi/3]$ or as $\beta_1 \in [-\beta_2, +2\pi/3]$, $\beta_2 \in [-2\pi/3, +2\pi/3]$, both with $\chi, \phi \in [0, 2\pi]$, and $\theta \in [0, \pi]$.

It can be seen geometrically or algebraically that if the particular values β_1^a and β_2^a are chosen so that the pair of bending angles

(β_1^a, β_2^a) defined by $\beta_1^a = \beta_1^c$ and $\beta_2^a = \beta_2^c$ fall in the allowed coordinate ranges for β_1 and β_2 specified above, then the pair (β_1^b, β_2^b) defined by $\beta_1^b = \beta_2^c$ and $\beta_2^b = \beta_1^c$ also fall within the allowed ranges for β_1 and β_2 . The exchange $\beta_1 \leftrightarrow \beta_2$ is thus permitted everywhere in the upper triangle of Fig. 1c, and the three non-identity elements of the PI group G_4 for this single-valued coordinate system can be taken, in the notation of Table 5 of [1], to be

$$(ab)(12)f(\beta_1, \beta_2, \chi, \theta, \phi) = C_2(y)f(\beta_1, \beta_2, \chi, \theta, \phi) = f(\beta_2, \beta_1, \pi - \chi, \pi - \theta, \pi + \phi), \quad (4a)$$

$$(ab)(12)^*f(\beta_1, \beta_2, \chi, \theta, \phi) = if(\beta_1, \beta_2, \chi, \theta, \phi) = f(\beta_2, \beta_1, \chi, \theta, \phi), \quad (4b)$$

$$E^*f(\beta_1, \beta_2, \chi, \theta, \phi) = \sigma(xz)f(\beta_1, \beta_2, \chi, \theta, \phi) = f(\beta_1, \beta_2, \pi - \chi, \pi - \theta, \pi + \phi). \quad (4c)$$

The mathematical meaning of these transformations, consistent with the definitions in [1], is such [5] that when $(ab)(12)$ acts on a function f of the five coordinates above; it replaces the symbol β_1 by the symbol β_2 everywhere that β_1 originally occurred in f ; it replaces the symbol β_2 by the symbol β_1 everywhere that β_2 originally occurred in f ; it replaces the symbol χ by $\pi - \chi$ everywhere in f ; etc. For example, from Eq. (4a) we find that $(ab)(12)[(\beta_1 + 1)(2 - \beta_2)^2(3 - \chi)^3] = [(\beta_2 + 1)(2 - \beta_1)^2(3 - \pi + \chi)^3]$. The latter expression can be rearranged (if desired) to give $[(2 - \beta_1)^2(\beta_2 + 1)(3 - \pi + \chi)^3]$, where the variables again appear in their original order. Symmetry species in the PI group G_4 can be labeled in various ways; we use the labels $A_g, A_u, B_g,$ and B_u given in Table 1a of [1].

We note in passing that a slight inconvenience of the coordinate system in the present section arises because the range of β_2 depends on the value of β_1 (or vice versa), which leads to non-constant limits in the integration scheme for matrix elements, e.g.,

$$\int_{\beta_1=-2\pi/3}^{+2\pi/3} \int_{\beta_2=-\beta_1}^{+2\pi/3} d\beta_1 d\beta_2. \quad (5)$$

Discussions of the coordinate ranges appropriate for the lower right triangle in Fig. 1c, or for the lower left or upper right triangles shown in Fig. 1d, would be very similar to that given above. They are not presented here.

Baraban has pointed out [6], though we have not investigated the resulting coordinate system in detail here, that it should also

be possible to use an hour glass shape for the allowed β_1, β_2 ranges of a single-valued coordinate system. In this scheme, the full length of both diagonals in the square would be used as boundary lines, and one would keep only the top and bottom isosceles triangles, which touch at a point in the center (or equivalently, keep only the left and right isosceles triangles).

3. Boundary conditions when only two bending LAMs are feasible

It is well known that it is the imposition of boundary conditions on solutions to Schrödinger's equation that leads to the quantization of bound energy levels. Nevertheless, boundary conditions are often not considered explicitly in modern molecular spectroscopy papers, because appropriate boundary conditions and their quantization effects have been worked out nearly a century ago for eigenfunctions of most of the zeroth-order Hamiltonians used to generate commonly used basis sets. When treating molecules with LAMs, however, one is sometimes tempted (as here) to use more unusual coordinates, as in Fig. 1a–d, and one must therefore reconsider the question of boundary conditions.

3.1. Boundary conditions used in Ref. [1] for the double-valued coordinates in Fig. 1a

Since the (somewhat arbitrarily chosen) limits of $\pm 2\pi/3$ for β_1 and β_2 are designed simply to stop each C–H bond from “rotating through the C–C bond” (see Fig. 3a of [1]), it is physically reasonable to require that $\Psi \rightarrow 0$ as it approaches each of the four edges $\beta_1 = -2\pi/3$, $\beta_1 = +2\pi/3$, $\beta_2 = -2\pi/3$, and $\beta_2 = +2\pi/3$ of the square in Fig. 1a. This specifies the boundary conditions on all four edges of the square in Fig. 1a. (We note in passing that the β_1, β_2 coordinate cutoffs could be moved much closer to $\pm\pi$, but they cannot be extended beyond those values, since then the large-amplitude bending motion would permit the H atoms to pass through the C–C bond.)

Because of our desire to avoid the complications associated with linear configurations, we also require that $\Psi \rightarrow 0$ as it approaches the dotted circle in Fig. 1a. Note that all boundary conditions here take the simple form that $\Psi \rightarrow 0$ where the potential $V \rightarrow \infty$.

3.2. Boundary conditions for use with the single-valued coordinates in Fig. 1b

We can again require that $\Psi \rightarrow 0$ as it approaches any of the three edges $\beta_1 = +2\pi/3$, $\beta_2 = -2\pi/3$, or $\beta_2 = +2\pi/3$ of the upper rectangle in Fig. 1b. However, the boundary conditions on the edge with $\beta_1 = 0$ are not obvious, and the author, using the methods in the next section, was not able to determine them, presumably because of the missing $\beta_1 \leftrightarrow \beta_2$ operation in the group theory. We do not describe these unsuccessful attempts.

3.3. Boundary conditions for use with the single-valued coordinates in Fig. 1c

We will not discuss boundary conditions for Fig. 1c from the point of view of some multidimensional numerical integration scheme for Schrödinger's partial differential equation, since understanding boundary conditions from this point of view proved to be difficult. Instead we look into boundary conditions on a set of basis functions that could be used to set up a Hamiltonian matrix, which is then diagonalized. The main reason for taking the second approach is that the boundary conditions turn out to be dependent on the rotational quantum number K_a , which is well characterized

in the basis functions, but not necessarily in the eigenfunctions after diagonalization.

We take products of the form $\lfloor_{K_a K_c} \rfloor f(\beta_1, \beta_2)$ as LAM basis functions for this problem, where $\lfloor_{K_a K_c} \rfloor$ is an ordinary asymmetric-rotor rotational function and $f(\beta_1, \beta_2)$ is an as yet uncharacterized basis function of the bending angles. The variable transformation associated with the symmetry operation $(ab)(12)^* = i$ from Eq. (4b), together with the character $\chi_{G_4}(i)$ for this operation when applied to a function of given symmetry species in G_4 , can be used to show that $f(\beta_1, \beta_2)$ must be either even or odd with respect to the $\beta_1 \leftrightarrow \beta_2$ exchange.

$$i\Psi(\beta_1, \beta_2, \chi, \theta, \phi) = \Psi(\beta_2, \beta_1, \chi, \theta, \phi) \\ = \chi_{G_4}(i)\Psi(\beta_1, \beta_2, \chi, \theta, \phi), \quad (6a)$$

$$i\lfloor_{K_a K_c} \rfloor f(\beta_1, \beta_2) = \lfloor_{K_a K_c} \rfloor f(\beta_2, \beta_1) = \chi_{G_4}(i)\lfloor_{K_a K_c} \rfloor f(\beta_1, \beta_2). \quad (6b)$$

Eqs. (6a) and (6b) represent, respectively, application of the symmetry operation i from Table 5 of [1] to a final bending-rotational eigenfunction Ψ and to a bending-rotational basis function. All characters in G_4 are either +1 or –1, and we can cancel $\lfloor_{K_a K_c} \rfloor \neq 0$ from both sides of Eq. (6b) to obtain

$$f(\beta_2, \beta_1) = \pm f(\beta_1, \beta_2), \quad (7)$$

where the + or – sign is given by the character of i to which the bending-rotational basis function belongs.

Even though the symmetry operation in Eq. (7) applies to all points β_1, β_2 in the upper left triangle in Fig. 1c, it nevertheless resembles a boundary condition. This is one of the important ideas in the present work, since it allows us to understand the relation between symmetry operations in multiple-valued coordinate systems and boundary conditions in single-valued coordinate systems. Its essence can be stated in words as follows. When some part of either or both of the diagonals of the square in Fig. 1a (shown as dashed lines in Figs. 1c and 1d) lies within the allowed range of the β_1, β_2 variables for the coordinate system under consideration, then reflection in the included diagonal forms a symmetry operation for that coordinate system, leading to even or odd behavior of allowed wavefunctions under reflection in the included diagonal. This even (or odd) reflection behavior leads in turn to the wavefunction crossing the included diagonal with a zero derivative (or a zero value). On the other hand, when either of these diagonals forms a boundary of the allowed range of the β_1, β_2 variables for the coordinate system under consideration, then the boundary conditions that must be imposed are that the wavefunction must have either a zero derivative or a zero value on this diagonal.

To demonstrate these remarks mathematically, we use the \pm signs in Eq. (7) as subscripts on f and change to symmetrized bending variables of the form

$$\beta_+ = (1/\sqrt{2})(\beta_1 + \beta_2), \\ \beta_- = (1/\sqrt{2})(\beta_1 - \beta_2). \quad (8)$$

We can then write

$$f_{\pm}(\beta_+, -\beta_-) = \pm f_{\pm}(\beta_+, \beta_-), \quad (9a)$$

$$f_+(\beta_+, \beta_-) = f_+^{(0)}(\beta_+, 0) + (1/2!)f_+^{(2)}(\beta_+, 0)\beta_-^2 \\ + (1/4!)f_+^{(4)}(\beta_+, 0)\beta_-^4 + \dots, \quad (9b)$$

$$f_-(\beta_+, \beta_-) = f_-^{(1)}(\beta_+, 0)\beta_- + (1/3!)f_-^{(3)}(\beta_+, 0)\beta_-^3 + \dots, \quad (9c)$$

where Eq. (9a) essentially defines another notation for describing the information in Eq. (7), and Eqs. (9b) and (9c), respectively, represent Taylor expansions of the even and odd functions in powers of β_- in the vicinity of $\beta_- = 0$, i.e., Taylor expansions in the vicinity of

the line $\beta_1 = \beta_2$ within the upper left triangle of Fig. 1c along a direction perpendicular to that line. The $f_+^{(n)}(\beta_+, 0)$ symbols are n^{th} derivatives along a direction perpendicular to the $\beta_1 = \beta_2$ line, evaluated at position β_+ on that line. The analogy with boundary conditions arises because $f_+^{(0)}(\beta_+, 0) \neq 0$, but $f_+^{(1)}(\beta_+, 0) = 0$, while $f_-^{(0)}(\beta_+, 0) = 0$, but $f_-^{(1)}(\beta_+, 0) \neq 0$, i.e., for both f_+ and f_- , either the function itself, or its first derivative across the $\beta_1 = \beta_2$ line, must vanish on that line.

We now turn to a consideration of the actual boundary conditions. For the upper left triangle in Fig. 1c, it is possible to use the simple boundary condition that $\Psi \rightarrow 0$ on two of the three edges, i.e., when either β_1 or $\beta_2 = +2\pi/3$. Boundary conditions on the long side of the triangle, with $\beta_1 = -\beta_2$ (or alternatively expressed, on the line with $\beta_+ = 0$) must be determined from other considerations as follows. The operation E_b from Table 5 of [1] is a limited identity, meaning that it does not change the positions of the four acetylene atoms in the laboratory, but it does change some of the molecule-fixed coordinates in Eq. (1), namely β_1 and β_2 are replaced by their negatives and χ is replaced by $\pi + \chi$. Thus, for some arbitrary total wavefunction $\Psi(\beta_1, \beta_2, \chi, \theta, \phi)$ we find

$$E_b \Psi(\beta_1, \beta_2, \chi, \theta, \phi) = \Psi(-\beta_1, -\beta_2, \pi + \chi, \theta, \phi) \\ = \Psi(\beta_1, \beta_2, \chi, \theta, \phi), \quad (10)$$

where the second equality follows [5] because E_b does not change atom positions in the laboratory, and a total wavefunction can always be written in terms of those atom positions. The transformation in Eq. (10) takes $\beta_1 + \beta_2$ outside of its allowed range of $\beta_1 + \beta_2 \geq 0$, but we can still use E_b and Eq. (10) to formally define Ψ at all points in the lower right triangle in Fig. 1c (where $\beta_1 + \beta_2 < 0$). Similarly, to extend the definition of a total bending-rotational basis function to the lower right triangle we write

$$E_b \mathbb{J}_{K_a K_c} f(\beta_1, \beta_2) = (-1)^{K_a} \mathbb{J}_{K_a K_c} f(-\beta_1, -\beta_2) \\ = + \mathbb{J}_{K_a K_c} f(\beta_1, \beta_2). \quad (11)$$

Canceling $\mathbb{J}_{K_a K_c}$ from both sides of the second equality in Eq. (11) we obtain Eq. (12a) for the bending basis function alone.

$$f(\beta_1, \beta_2) = +(-1)^{K_a} f(-\beta_1, -\beta_2), \quad (12a)$$

$$f(\beta_1, \beta_2) = +\chi_{G_4}(i) (-1)^{K_a} f(-\beta_2, -\beta_1). \quad (12b)$$

Eq. (12a) indicates that $f(\beta_1, \beta_2)$, when its definition is extended to cover all values in the range $\beta_1, \beta_2 \in [-2\pi/3, +2\pi/3]$, must be even or odd with respect to inversion in the origin, depending on whether K_a is even or odd, respectively. Eq. (12b), which is needed below, follows from Eq. (6b).

Rewriting Eq. (12b) in a notation similar to that used in Eq. (9) yields

$$f_{\pm}(-\beta_+, \beta_-) = \pm f_{\pm}(\beta_+, \beta_-), \quad (13a)$$

$$f_+(\beta_+, \beta_-) = f_+^{(0)}(0, \beta_-) + (1/2!) f_+^{(2)}(0, \beta_-) \beta_+^2 \\ + (1/4!) f_+^{(4)}(0, \beta_-) \beta_+^4 + \dots, \quad (13b)$$

$$f_-(\beta_+, \beta_-) = f_-^{(1)}(0, \beta_-) \beta_+ + (1/3!) f_-^{(3)}(0, \beta_-) \beta_+^3 + \dots, \quad (13c)$$

where the symbols have different meanings from those in Eq. (9), i.e., the \pm subscripts on f now reflect the sign in Eq. (12b), and the derivatives are now to be taken at a position β_- on the line $\beta_+ = 0$ in a direction perpendicular to this line. The boundary conditions implied by Eqs. (13b) and (13c) on the line $\beta_+ = 0$ (or alternatively expressed, on the line $\beta_1 = -\beta_2$) are now that $f_+^{(0)}(0, \beta_-) \neq 0$, but $f_+^{(1)}(0, \beta_-) = 0$, while $f_-^{(0)}(0, \beta_-) = 0$, but $f_-^{(1)}(0, \beta_-) \neq 0$, i.e., either the function f_+ or f_- itself, or its derivative across the $\beta_1 = -\beta_2$ line, vanishes on that line.

These boundary conditions on the $\beta_+ = 0$ line could have been anticipated from the symmetry relations at the $\beta_- = 0$ line in Eqs. (9a)–(9c), since we could have chosen to work with the lower left triangle in Fig. 1d instead of the upper left triangle in Fig. 1c, which effectively interchanges the roles of the $\beta_1 = +\beta_2$ and $\beta_1 = -\beta_2$ lines.

The results of Eqs. (7) and (12), including the dependence on $\chi_{G_4}(i)$ and $(-1)^{K_a}$, are summarized in Table 1, using an expanded notation $f_{\pm\pm}(\beta_1, \beta_2)$, where the first \pm subscript indicates the behavior in Eqs. (7) and (9a), and the second, independent, \pm subscript indicates the behavior in Eqs. (12b) and (13a).

4. Comparison of the boundary conditions obtained for a single-valued coordinate system with those obtained for a double-valued coordinate system

We now indicate (in rather condensed fashion) how the $G_4^{(2)}$ double-group treatment in Section 3.1 of the acetylene LAM tunneling problem using a double-valued coordinate system gives the same restrictions involving K_a , and $\chi_{G_4}(i)$ on the boundary conditions for $f(\beta_1, \beta_2)$ as are obtained from the G_4 treatment in Section 3.3 of this same tunneling problem using a single-valued coordinate system. Table 2 gives, as preliminary information, the species in $G_4^{(2)}$ of the $\mathbb{J}_{K_a K_c}$ asymmetric top functions and the $f_{\pm\pm}(\beta_1, \beta_2)$ bending functions, as well as the species in $G_4^{(2)}$ that have the same character in G_4 (either +1 or -1) for both of the $(ab)(12)^*$ operations in $G_4^{(2)}$. These are the single-valued representations [1] of the double group $G_4^{(2)}$ to which the total (here, bending-rotational) wavefunctions must belong [5].

Table 3 then gives subscripts and $G_4^{(2)}$ symmetry species ${}^b\Gamma$ of the bending functions $f_{\pm\pm}(\beta_1, \beta_2)$ that are allowed to multiply rotational functions having the $G_4^{(2)}$ rotational symmetry species ${}^r\Gamma$ (from Table 2) indicated at the left of Table 3, when the overall $G_4^{(2)}$ bending-rotational symmetry species (from Table 2) is that indicated at the top of Table 3. Table 3 is the analog of Table 1, and the same rules are found in both tables, showing that the results from the treatment in [1] using a double-valued coordinate system are the same as those obtained in Section 3.3 using a single-valued coordinate system.

As a final point, consider symmetry species for the basis functions in the two treatments. Asymmetric rotor rotational basis functions $\mathbb{J}_{K_a K_c}$ only belong to one of the two symmetry species A_g or B_g in the PI group G_4 defined in Eq. (4) for the single-valued coordinate system, whereas $\mathbb{J}_{K_a K_c}$ can belong to one of the four species A_{gs}, B_{gs}, A_{gd} or B_{gd} in $G_4^{(2)}$. Similarly, the bending basis functions $f_{\pm\pm}(\beta_1, \beta_2)$ only belong to one of the two symmetry species A_g or B_u in the PI group G_4 defined in Eq. (4) for the single-valued coordinate system, whereas the $f_{\pm\pm}(\beta_1, \beta_2)$ can belong to one of the four species A_{gs}, B_{us}, A_{gd} or B_{ud} in $G_4^{(2)}$. This means, for example, that the single-valued coordinate treatment associated with Fig. 1c is unable to distinguish by group-theoretical means $f_{\pm\pm}(\beta_1, \beta_2)$ functions that vanish on the long boundary of the triangle in Fig. 1c from those that do not. This (in the author's opinion) is an undesirable symmetry deficiency of the single-valued coordinate treatment.

Table 1
Symmetry properties^a required for the functions $f_{\pm\pm}(\beta_1, \beta_2)$ as a function of $\chi_{G_4}(i)^b$ and K_a^b .

$\chi_{G_4}(i)^b$	$K_a^b = \text{even}$	$K_a^b = \text{odd}$
+1	++	+-
-1	--	-+

^a Symmetry properties indicated in this table are the changes in sign of $f_{\pm\pm}(\beta_1, \beta_2)$ with respect to $\beta_1 \leftrightarrow \beta_2$ (first subscript) and $\beta_1 \leftrightarrow -\beta_2$ (second subscript).

^b $\chi_{G_4}(i)$ is the character of the basis function $\mathbb{J}_{K_a, J, M} f(\beta_1, \beta_2)$ under the operation i of the PI group, and K_a is the a -axis rotational projection quantum number in this basis function.

Table 2

Top half: symmetry species in $G_4^{(2)}$ of the rotational (${}^r\Gamma$) and bending (${}^b\Gamma$) basis functions. Bottom half: species in $G_4^{(2)}$ that correlate with $\chi_{C_4}(i) = \pm 1$, where $i = (ab)(12)^*$ in G_4 .

$K_a K_c^a$	${}^r\Gamma$	$f_{\pm\pm}(\beta_1, \beta_2)^b$	${}^b\Gamma$
ee	A_{gs}	++	A_{gs}
eo	B_{gs}	+-	A_{gd}
oe	A_{gd}	-+	B_{ud}
oo	B_{ud}	--	B_{us}
$\chi_{C_4}(i)$	Γ in $G_4^{(2)c}$		
+1	$A_{gs} \oplus B_{gs}$		
-1	$A_{us} \oplus B_{us}$		

^a The (e)ven or (o)dd character of the usual K_a , K_c asymmetric rotor quantum numbers.

^b The first sign indicates whether $f \rightarrow +f$ or $-f$ when $\beta_1 \leftrightarrow \beta_2$; the second sign indicates whether $f \rightarrow +f$ or $-f$ when $\beta_1 \leftrightarrow -\beta_2$.

^c These are the species in $G_4^{(2)}$ that have the character indicated under $\chi_{C_4}(i)$ for both $(ab)(12)^*$ operations. Total rotation-bending wave functions or total basis functions can only belong to such "single-valued" representations (subscript s in Table 6 of [1]).

Table 3

Bending functions $f_{\pm\pm}(\beta_1, \beta_2)$ that are compatible in $G_4^{(2)}$ with the K_a and bending-rotational species indicated.

K_a^a	${}^r\Gamma$	${}^b\Gamma = A_{gs} \oplus B_{gs}^b$		${}^b\Gamma = A_{us} \oplus B_{us}^c$	
		subs ^d	${}^b\Gamma^d$	subs ^d	${}^b\Gamma^d$
e	A_{gs}	++	A_{gs}	--	B_{us}
e	B_{gs}	++	A_{gs}	--	B_{us}
o	A_{gd}	+-	A_{gd}	-+	B_{ud}
o	B_{gd}	+-	A_{gd}	-+	B_{ud}

^a Rotational symmetry species ${}^r\Gamma$ are shown for e(ven) and (o)dd K_a .

^b Species in $G_4^{(2)}$ with $\chi_{C_4}[(ab)(12)^*] = +1$.

^c Species in $G_4^{(2)}$ with $\chi_{C_4}[(ab)(12)^*] = -1$.

^d Subscripts and species ${}^b\Gamma$ of the $f_{\pm\pm}(\beta_1, \beta_2)$ which, when multiplied by ${}^r\Gamma$ give the bending-rotational symmetry species in the column headings.

5. Examples of computed LAM bending wavefunctions

Baraban et al. [3] have used an ab initio potential surface for the S_1 electronic state and a reduced dimension discrete variable representation calculation to compute numerical bending vibrational wavefunctions in S_1 up to energies exceeding 15000 cm^{-1} . In particular, Fig. 2 of [3] (see the web version in color) illustrates nicely the four symmetry species in $G_4^{(2)}$ available for the bending functions. The first \pm subscript on $f_{\pm\pm}(\beta_1, \beta_2)$ here indicates even or odd behavior under reflection in the principal diagonal (upper left to lower right) in their Fig. 2, while the second \pm subscript indicates even or odd behavior about the other diagonal. In the notation of Table 6 of [1], the symmetry species in $G_4^{(2)}$ of the four wavefunctions shown (proceeding clockwise from the upper left) are A_{gd} , A_{gs} , B_{ud} , and B_{us} .

As expected from tunneling considerations [1], Baraban et al. find [3,6], again in the notation of [1], that bending functions located mainly in the trans wells occur in nearly degenerate A_{gs} , A_{gd} or B_{us} , B_{ud} pairs, while bending functions located mainly in the cis wells occur in nearly degenerate A_{gs} , B_{ud} or A_{gd} , B_{us} pairs, but the accuracy of the computational method at the moment does not appear to be high enough [6] to give reliable values for the tunneling splittings.

It would obviously be of interest to compare in detail, once the computational accuracy improves somewhat, bending energy levels and bending wavefunctions calculated using a double-valued coordinate system containing two trans and two cis wells (as was done in [3]) with energy levels and wavefunctions calculated using some single-valued coordinate system containing only one trans and one cis well. The considerations of this paper indicate

that these conceptually different calculations should give the same numerical results.

6. Changes that occur when internal rotation is added to the local bends as a third feasible LAM

The changes in various equations and associated group theory that are necessary when a third LAM is added are as follows. The equation relating laboratory-fixed and molecule-fixed coordinates becomes [1]

$$\mathbf{R}_i = \mathbf{R} + S^{-1}(\chi, \theta, \phi)[\mathbf{a}_i(\alpha, \beta_1, \beta_2) + \mathbf{d}_i], \quad (14)$$

where the new variable α is an internal rotation angle describing equal and opposite rotations of the $H_1-C_a-C_b$ and $C_a-C_b-H_2$ groups about the C_a-C_b bond (which is taken to define the direction of the z axis). This definition of α has the effect of keeping the y axis along the C_2 symmetry axis of the molecule during this internal rotation, but it also causes the change in the $H_1-C_a-C_b-H_2$ dihedral angle to be $2\Delta\alpha$, rather than $\Delta\alpha$ itself.

6.1. Coordinate ranges and symmetry transformations used in Ref. [1] for Fig. 2a

Fig. 2a illustrates, in the form of a cube, the ranges of the LAM coordinates α , β_1 , and β_2 used in Ref. [1], i.e., $\alpha \in [0, 2\pi]$; $\beta_1, \beta_2 \in [-2\pi/3, +2\pi/3]$; $\chi, \phi \in [0, 2\pi]$; and $\theta \in [0, \pi]$. As discussed at length in Section 8 of [1], these molecule-fixed coordinates are octuple-valued, i.e., a given laboratory-fixed configuration (in which each of the four labeled acetylene atoms has a specified location in the laboratory) is described by eight different combinations of the molecule-fixed coordinates, i.e.,

$$\begin{bmatrix} \alpha^\circ \\ \beta_1^\circ \\ \beta_2^\circ \\ \chi^\circ \\ \theta^\circ \\ \phi^\circ \end{bmatrix}, \begin{bmatrix} \alpha^\circ \\ \beta_1^\circ \\ \beta_2^\circ \\ \chi^\circ + \pi \\ \theta^\circ \\ \phi^\circ \end{bmatrix}, \begin{bmatrix} \alpha^\circ + \pi \\ \beta_1^\circ \\ \beta_2^\circ \\ \chi^\circ + \pi \\ \theta^\circ \\ \phi^\circ \end{bmatrix}, \begin{bmatrix} \alpha^\circ + \pi \\ \beta_1^\circ \\ \beta_2^\circ \\ \chi^\circ \\ \theta^\circ \\ \phi^\circ \end{bmatrix}, \begin{bmatrix} \alpha^\circ + \pi/2 \\ \beta_1^\circ \\ \beta_2^\circ \\ \chi^\circ + \pi/2 \\ \theta^\circ \\ \phi^\circ \end{bmatrix},$$

$$\begin{bmatrix} \alpha^\circ + \pi/2 \\ \beta_1^\circ \\ \beta_2^\circ \\ \chi^\circ - \pi/2 \\ \theta^\circ \\ \phi^\circ \end{bmatrix}, \begin{bmatrix} \alpha^\circ - \pi/2 \\ \beta_1^\circ \\ \beta_2^\circ \\ \chi^\circ - \pi/2 \\ \theta^\circ \\ \phi^\circ \end{bmatrix} \text{ or } \begin{bmatrix} \alpha^\circ - \pi/2 \\ \beta_1^\circ \\ \beta_2^\circ \\ \chi^\circ + \pi/2 \\ \theta^\circ \\ \phi^\circ \end{bmatrix},$$

where a given symbol with superscript $^\circ$ again represents a fixed numerical value. Note that all of these coordinate sets have the same values for the rotational angles θ and ϕ , i.e., they all have their z axis pointing in the same direction in the laboratory.

The symmetry transformations applied to functions of these (unsubscripted) coordinates [5] and the character table of the resulting extended PI symmetry group $G_4^{(8)}$, containing 32 elements, are given in Tables 9 and 10 of [1]. The group $G_4^{(8)}$ is an eightfold extended group of the acetylene PI group G_4 , which, we recall, contains the PI operations E , $(ab)(12)$, $(ab)(12)^*$ and E^* . Because bond-breaking is not feasible, neither (ab) nor (12) can occur by itself in the PI group.

As indicated above, the coordinate ranges discussed in this section are those that were actually used in the multiple-valued group-theoretical treatment of Ref. [1]. Sections 6.2–6.5 give brief descriptions of some possibilities for restricting these ranges so as to produce a variety of single-valued coordinate systems, together with brief discussions of the changes in the group theory that occur when the ranges are restricted. Boundary conditions

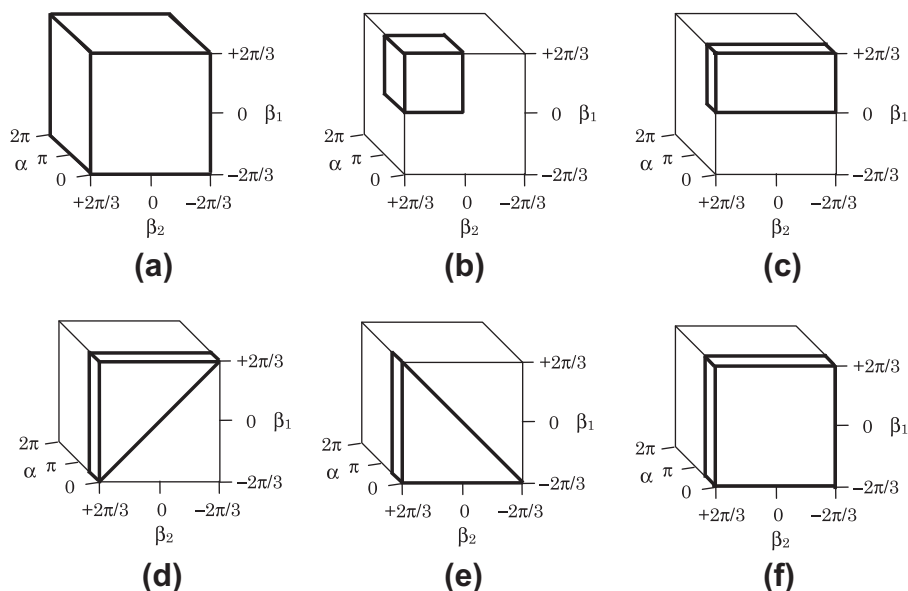


Fig. 2. Schematic depiction of coordinate ranges for the internal rotation angle α and the two local bending angles β_1 and β_2 in bent acetylene. The potential surface as a function of these three LAM coordinates is not shown. Except for Fig. 2f, the rotational variables have their usual ranges: $\chi, \phi \in [0, 2\pi]$ and $\theta \in [0, \pi]$. (a) The ranges shown for the LAM torsional and bending coordinates, $0 \leq \alpha \leq 2\pi$ and $-2\pi/3 \leq \beta_1, \beta_2 \leq +2\pi/3$, are those used in [1]. This coordinate domain is octuple-valued. It contains eight deeper trans wells and eight shallower cis wells, as well as a high barrier at the linear configuration. Boundary conditions require that $\Psi \rightarrow 0$ on the four faces of the cube characterized by $\beta_1, \beta_2 = -2\pi/3$ and $\beta_1, \beta_2 = +2\pi/3$, as well as a periodicity of 2π for α . (b) A smaller “cubic” domain for the LAM coordinates, with $0 \leq \alpha \leq \pi$ and $0 \leq \beta_1, \beta_2 \leq 2\pi/3$, that contains only one trans and one cis well and gives a single-valued coordinate system. These coordinate ranges exhibit the full PI symmetry of the problem. Boundary conditions require that $\Psi \rightarrow 0$ on the two faces characterized by $\beta_1, \beta_2 = +2\pi/3$, but boundary conditions for the other four faces must be determined from other considerations (see text). (c) A rectangular-slab domain for the LAM coordinates, with $0 \leq \alpha \leq \pi/2$, $0 \leq \beta_1 \leq 2\pi/3$, and $-2\pi/3 \leq \beta_2 \leq 2\pi/3$, that contains only one trans and one cis well and gives a single-valued coordinate system. These coordinate ranges do not exhibit the full PI symmetry of the problem. Boundary conditions require that $\Psi \rightarrow 0$ on the three faces characterized by $\beta_1, \beta_2 = +2\pi/3$ and $\beta_2 = -2\pi/3$, but not on the other three faces. (d) A triangular-slab domain for the LAM coordinates, with $0 \leq \alpha \leq \pi/2$, $-2\pi/3 \leq \beta_1 \leq +2\pi/3$ and $-\beta_1 \leq \beta_2 \leq +2\pi/3$, that contains one trans and one cis well and gives a single-valued coordinate system, but does not exhibit the full PI symmetry of the problem. Boundary conditions require that $\Psi \rightarrow 0$ on the faces characterized by $\beta_1, \beta_2 = +2\pi/3$, but not on the other three faces. (e) An alternative triangular domain, with $0 \leq \alpha \leq \pi/2$, $-2\pi/3 \leq \beta_1 \leq +2\pi/3$ and $+\beta_1 \leq \beta_2 \leq +2\pi/3$, with properties very similar to Fig. 1d. (f) A square-slab domain, with $0 \leq \alpha \leq \pi/2$ and $-2\pi/3 \leq \beta_1, \beta_2 \leq +2\pi/3$, that contains two trans and two cis wells and gives a single-valued coordinate system only if the traditional range of the rotational angle χ is cut in half, i.e., if $0 \leq \chi \leq \pi$. Coordinate systems that deviate from traditional rotational angle definitions are not considered here.

(of varying complexity) for these same coordinate ranges are discussed separately in Section 7. Section 8 then turns to an illustration of the main point of this paper, i.e., the simple boundary conditions that must be imposed on wavefunctions in the multiple-valued coordinate system of Fig. 2a, together with the coordinate transformations corresponding to extended-group symmetry operations there, are equivalent to the more complicated boundary conditions that must be imposed on wavefunctions in the single-valued coordinate system of Fig. 2b.

6.2. Coordinate ranges and symmetry transformations for use with Fig. 2b

Fig. 2b illustrates, in the form of a smaller cube, one choice for ranges for the LAM coordinates α , β_1 , and β_2 that have been restricted to give a single-valued molecular coordinate system. These restricted ranges are $\alpha \in [0, \pi]$ and $\beta_1, \beta_2 \in [0, +2\pi/3]$. The ranges of the rotational coordinates remain unchanged: $\chi, \phi \in [0, 2\pi]$ and $\theta \in [0, \pi]$. Since β_1 and β_2 take only positive values in the small cube of Fig. 2b, each of these angles now corresponds to the traditional bending angle in a triatomic molecule, which also takes only positive values. Furthermore, since there were originally eight points within the large cube which all corresponded to exactly the same laboratory configuration, it seems reasonable that a cube one-eighth the size of the large cube would eliminate the redundancy in the molecule-fixed coordinates. This can be verified by noting that the last seven sets of coordinates given in Section 6.1 all fall outside the small cube, if the first set lies within that cube.

Note that the range of α had to be cut in half in Fig. 2b, so that each “chiral” form of an internally rotated trans-bent acetylene with labeled atoms will occur only once as α traverses its allowed

domain, i.e., as the molecule passes through the forms trans \rightarrow cis \rightarrow trans. This $[0, \pi]$ range for α causes the dihedral angle now to have a range of only $[0, 2\pi]$, so 2π periodicity in the internal rotation coordinate could be regained by switching from α to a conventionally defined dihedral angle. (We do not do this here, however, to avoid deviating from the coordinate definitions, and therefore also from the coordinate transformations given in [1].)

Coordinate transformations that are permissible for the small cube in Fig. 2b can be selected from those given in Table 9 of [1] by noting that permitted transformations can exchange β_1 and β_2 , but must keep them both positive. Similarly, transformations that change α can only replace it by $\pi - \alpha$. Other transformations from Table 9 of [1] are not permitted, since replacement of α by $-\alpha$ or $\pi + \alpha$ always takes α outside its allowed range, and replacement by $+\pi/2 \pm \alpha$ or $-\pi/2 \pm \alpha$ sometimes takes α outside of its allowed range.

With these restrictions, we find for this single-valued coordinate system that the allowed symmetry group is, as expected, exactly the PI group G_4 , with transformations (apart from the identity) given, in the notation of Table 9 of [1], by

$$(ab)(12)f(\alpha, \beta_1, \beta_2, \chi, \theta, \phi) = a^2bf(\alpha, \beta_1, \beta_2, \chi, \theta, \phi) \\ = f(\alpha, \beta_2, \beta_1, \pi - \chi, \pi - \theta, \pi + \phi),$$

$$(ab)(12)^*f(\alpha, \beta_1, \beta_2, \chi, \theta, \phi) = a^2bcf(\alpha, \beta_1, \beta_2, \chi, \theta, \phi) \\ = f(\pi - \alpha, \beta_2, \beta_1, \pi + \chi, \theta, \phi),$$

$$E^*f(\alpha, \beta_1, \beta_2, \chi, \theta, \phi) = cf(\alpha, \beta_1, \beta_2, \chi, \theta, \phi) \\ = f(\pi - \alpha, \beta_1, \beta_2, -\chi, \pi - \theta, \pi + \phi). \quad (15)$$

The meaning of these transformations is as described following Eq. (4). The symmetry labels A_g , A_u , B_g , and B_u for G_4 are again taken from Table 1a of [1].

Symmetry species of various basis functions in the G_4 group above are as follows. Torsional basis functions divide into two groups: $\sin(2k+1)\alpha$ and $\cos(2k)\alpha$ are of species ${}^1\Gamma = A_g$ in G_4 , while $\cos(2k+1)\alpha$ and $\sin(2k)\alpha$ are of species A_u , where k is any integer. Bending basis functions also divide into two groups: $f(\beta_1, \beta_2) + f(\beta_2, \beta_1)$ are of species ${}^b\Gamma = A_g$, while $f(\beta_1, \beta_2) - f(\beta_2, \beta_1)$ are of species B_u . Asymmetric-top basis functions J_{KaKc} divide into four groups: functions with $K_a K_c = ee, eo, oe, \text{ and } oo$, respectively, are of species ${}^r\Gamma = A_g, B_g, A_u, \text{ and } B_u$.

6.3. Coordinate ranges and symmetry transformations for use with Fig. 2c

Fig. 2c illustrates, in the form of a rectangle of finite thickness, another choice for restricted ranges of the LAM coordinates α , β_1 , and β_2 that give a single-valued molecular coordinate system. The coordinate ranges are $\alpha \in [0, \pi/2]$, $\beta_1 \in [0, +2\pi/3]$, and $\beta_2 \in [-2\pi/3, +2\pi/3]$, so that this rectangular “slab” again occupies one-eighth of the original cube. The ranges of the rotational coordinates remain unchanged. As for the two-LAM case, the unsymmetrical ranges for β_1 and β_2 mask the symmetry equivalence of the local bending modes at each end of the molecule, since it is no longer possible to exchange β_2 , which can have negative values, with β_1 , which must remain positive. Note that the range of α is now only one-fourth of its original value, so that the internally rotating molecule passes only through the forms $\text{trans} \rightarrow \text{cis}$.

Again, since there were originally eight points within the large cube which all corresponded to exactly the same laboratory configuration, it seems reasonable that a rectangular slab occupying one-eighth the volume of the large cube would eliminate the redundancy in the molecule-fixed coordinates. This can be verified by noting that the last seven sets of coordinates given in Section 6.1 all fall outside the slab, if the first set lies within it.

Coordinate transformations that are permissible for the rectangular slab in Fig. 2c can be selected from those given in Table 9 of [1] by noting that permitted transformations cannot exchange β_1 and β_2 , and cannot make β_1 negative. Transformations that change α can only replace it by $\pi/2 - \alpha$. With these restrictions, we find, as expected by analogy with Section 2.2, that the PI group for this single-valued coordinate system contains only the two elements E and E^* . The action of E^* on a function, in the notation of Table 9 of [1], is given by

$$\begin{aligned} E^*f(\alpha, \beta_1, \beta_2, \chi, \theta, \phi) &= abf(\alpha, \beta_1, \beta_2, \chi, \theta, \phi) \\ &= f(\pi/2 - \alpha, \beta_1, -\beta_2, 3\pi/2 - \chi, \pi - \theta, \\ &\quad \pi + \phi), \end{aligned} \quad (16)$$

6.4. Coordinate ranges and symmetry transformations for use with Figs. 2d and 2e

Fig. 2d indicates, in the form of a triangle of finite thickness, a restricted coordinate range having $\alpha \in [0, \pi/2]$, $\beta_1 \in [-2\pi/3, +2\pi/3]$, and $\beta_2 \in [-\beta_1, +2\pi/3]$. As in Section 2.3, we recover the $\beta_1 \leftrightarrow \beta_2$ coordinate transformation, but we still cannot use the full G_4 permutation-inversion group for this single-valued coordinate system, since the only useable non-identity symmetry operation from Table 9 of [1] becomes

$$\begin{aligned} (ab)(12)f(\alpha, \beta_1, \beta_2, \chi, \theta, \phi) &= a^2bf(\alpha, \beta_1, \beta_2, \chi, \theta, \phi) \\ &= f(\alpha, \beta_2, \beta_1, \pi - \chi, \pi - \theta, \pi + \phi). \end{aligned} \quad (17)$$

One can attempt to recover the full G_4 permutation-inversion group by, for example, shifting the $\pi/2$ range of the internal rotation angle to $\alpha \in [-\pi/4, +\pi/4]$, so that $\alpha \rightarrow -\alpha$ is a permissible coordinate transformation, but then the cis conformation cannot be reached. Other attempts lead to other difficulties.

Fig. 2e indicates an alternate triangular slab coordinate range lying within Fig. 2a. Discussion of Fig. 2e parallels that for Fig. 2d.

6.5. Coordinate ranges and symmetry transformations for use with Fig. 2f

Fig. 2f illustrates, in the form of a square slab, still another choice for ranges for the LAM coordinates α , β_1 , and β_2 that give a single-valued molecular coordinate system, namely $\alpha \in [0, \pi/2]$ and $\beta_1, \beta_2 \in [-2\pi/3, +2\pi/3]$. But this time, the range of the rotational coordinate χ does not remain unchanged, i.e., $\chi \in [0, \pi]$, since the range for χ must be cut in half to avoid coordinate redundancy as soon as positive and negative values are allowed for both local bending angles. It is not possible to cut the range for α in half compared to that in Fig. 2c, because then half of the non-planar configurations would be unreachable.

For very floppy molecules, whose rotational levels have little or no relation to those of a rigid rotor, coordinate systems that abandon the use of traditional Eulerian angles might be advantageous, but for the present C_2H_2 problem one is reluctant to give up the use of symmetric top basis functions and all of the algebra associated with three-dimensional angular momentum theory, so Fig. 2f is presented here more as a curiosity than as a useful suggestion.

Fig. 2f does permit, however, choosing symmetry transformations from Table 9 of [1] corresponding to the full PI group G_4 , since the full positive and negative ranges of both β_1 and β_2 make all their transformations possible again. If the ranges for α and χ are slightly shifted to the more symmetric intervals $\alpha \in [-\pi/4, +\pi/4]$ and $\chi \in [-\pi/2, +\pi/2]$, which permit α to be replaced by $-\alpha$ and χ to be replaced by $-\chi$, then the three operations corresponding to those in Eq. (15) above become

$$\begin{aligned} (ab)(12)f(\alpha, \beta_1, \beta_2, \chi, \theta, \phi) &= bf(\alpha, \beta_1, \beta_2, \chi, \theta, \phi) \\ &= f(\alpha, -\beta_2, -\beta_1, -\chi, \pi - \theta, \pi + \phi), \\ (ab)(12)^*f(\alpha, \beta_1, \beta_2, \chi, \theta, \phi) &= a^2bcdf(\alpha, \beta_1, \beta_2, \chi, \theta, \phi) \\ &= f(-\alpha, \beta_2, \beta_1, \chi, \theta, \phi), \\ E^*f(\alpha, \beta_1, \beta_2, \chi, \theta, \phi) &= a^2cdf(\alpha, \beta_1, \beta_2, \chi, \theta, \phi) \\ &= f(-\alpha, -\beta_1, -\beta_2, -\chi, \pi - \theta, \pi + \phi). \end{aligned} \quad (18)$$

7. Boundary conditions when three LAMs are feasible

7.1. Boundary conditions used in Ref. [1] for the octuple-valued coordinates of Fig. 2a

As mentioned earlier, the limits of $\pm 2\pi/3$ for β_1 and β_2 are designed to stop each C–H bond from “rotating through the C–C bond,” so we again require that $\Psi = 0$ on each of the four faces of the cube in Fig. 2a where V is assumed to be infinite, i.e., on the $\beta_1 = -2\pi/3$ (bottom), $\beta_1 = +2\pi/3$ (top), $\beta_2 = -2\pi/3$ (right), and $\beta_2 = +2\pi/3$ (left) faces.

The allowed range for a single-valued internal-rotation coordinate should be $0 \leq \alpha < 2\pi$, since points at $\alpha \pm 2\pi$ in Eq. (14) represent exactly the same laboratory configurations for $H_1-C_a-C_b-H_2$ as the corresponding points at α do. We thus require Ψ on the $\alpha = 2\pi$ (back) face to be equal to Ψ on the $\alpha = 0$ (front) face of the large cube in Fig. 2a. This 2π periodicity is automatically

accomplished by the choice in [1] of basis functions for the internal rotation motion of the form $e^{\pm im\alpha}$ with integer m .

The two paragraphs above specify the rather simple boundary conditions on all six faces of the cube in Fig. 2a.

7.2. Boundary conditions for use with the single-valued coordinates of Fig. 2b

We can again require that $\Psi \rightarrow 0$ as it approaches either of the two faces $\beta_1 = +2\pi/3$ (top) or $\beta_2 = +2\pi/3$ (left) of the small cube in Fig. 2b. Extensive algebraic manipulations are required to find out what the boundary conditions on the other four faces should be. We start by taking basis functions of the form

$$|K_a, J, M\rangle e^{+im\alpha} f(\beta_1, \beta_2), \quad (19)$$

where $|K_a, J, M\rangle \equiv (4\pi)^{-1/2} D_{K_a, M}^J(\chi, \theta, \phi)$ represents a Wigner [7] symmetric top wavefunction, m is an integer, and $f(\beta_1, \beta_2)$ represents some as yet unspecified function of the local mode bending angles.

7.2.1. Boundary conditions for the $\alpha = 0$ and $\alpha = \pi$ boundary faces in Fig. 2b

The operation d from Table 9 of [1] is a limited identity, since it does not change the positions of the four acetylene atoms in the laboratory, but it does change some of the molecule-fixed coordinates in Eq. (14), namely α and χ are replaced, respectively, by $\pi + \alpha$ and $\pi + \chi$. Thus, for some arbitrary total wavefunction $\Psi(\alpha, \beta_1, \beta_2, \chi, \theta, \phi)$ we find

$$d\Psi(\alpha, \beta_1, \beta_2, \chi, \theta, \phi) = \Psi(\pi + \alpha, \beta_1, \beta_2, \pi + \chi, \theta, \phi). \quad (20)$$

In general, this transformation is not useful for Fig. 2b, because it takes α outside of its allowed range of $[0, \pi]$. But if we set $\alpha = 0$ in Eq. (20), we see that d can be used to convert Ψ on the $\alpha = 0$ (front) boundary face of the small cube in Fig. 2b to Ψ on the $\alpha = \pi$ (back) boundary face. Since d is a limited identity, the two sets of molecule-fixed coordinates in Eq. (20) correspond to exactly the same laboratory configuration, and thus must correspond to exactly the same Ψ . From this we conclude that

$$\Psi(0, \beta_1, \beta_2, \chi, \theta, \phi) = \Psi(\pi, \beta_1, \beta_2, \pi + \chi, \theta, \phi). \quad (21)$$

When this relation between total wavefunctions on the $\alpha = 0$ and $\alpha = \pi$ boundary faces is applied to a basis function having the form given in Eq. (19) we find

$$|K_a, J, M\rangle f(\beta_1, \beta_2) = (-1)^{K_a+m} |K_a, J, M\rangle f(\beta_1, \beta_2), \quad (22)$$

which can only be satisfied if $K_a + m$ is an even integer, i.e., can only be satisfied if K_a and m are both even or both odd. This is the boundary condition that must be imposed on the basis functions as a result of considering the $\alpha = 0$ and $\alpha = \pi$ boundary faces in Fig. 2b.

7.2.2. Boundary conditions for the $\beta_1 = 0$ and $\beta_2 = 0$ boundary faces in Fig. 2b

The remaining two boundary faces, with $\beta_1 = 0$ (bottom) and $\beta_2 = 0$ (right) can be dealt with using logic similar to that in Section 3.3. Consider the equations obtained by applying the limited identities a^3bc and a^3bcd from Table 9 of [1] to a total wavefunction Ψ and to a basis function from Eq. (19)

$$\begin{aligned} a^3bc\Psi(\alpha, \beta_1, \beta_2, \chi, \theta, \phi) &= \Psi(\pi/2 + \alpha, -\beta_1, \beta_2, \\ &\quad -\pi/2 + \chi, \theta, \phi) \\ &= \Psi(\alpha, \beta_1, \beta_2, \chi, \theta, \phi), \end{aligned} \quad (23a)$$

$$\begin{aligned} a^3bcd\Psi(\alpha, \beta_1, \beta_2, \chi, \theta, \phi) &= \Psi(-\pi/2 + \alpha, -\beta_1, \beta_2, \\ &\quad \pi/2 + \chi, \theta, \phi) \\ &= \Psi(\alpha, \beta_1, \beta_2, \chi, \theta, \phi), \end{aligned} \quad (23b)$$

$$\begin{aligned} a^3bc|K_a, J, M\rangle e^{+im\alpha} f(\beta_1, \beta_2) &= (+i)^{m-K_a} |K_a, J, M\rangle e^{+im\alpha} f(-\beta_1, \beta_2) \\ &= |K_a, J, M\rangle e^{+im\alpha} f(\beta_1, \beta_2), \end{aligned} \quad (23c)$$

$$\begin{aligned} a^3bcd|K_a, J, M\rangle e^{+im\alpha} f(\beta_1, \beta_2) &= (-i)^{m-K_a} |K_a, J, M\rangle e^{+im\alpha} f(-\beta_1, \beta_2) \\ &= |K_a, J, M\rangle e^{+im\alpha} f(\beta_1, \beta_2). \end{aligned} \quad (23d)$$

In each of Eqs. (23a)–(23d), the wavefunction after the first equality is that obtained by carrying out the change of variables associated with the symmetry operation, while the wavefunction after the second equality is always the original wave function because both a^3bc and a^3bcd are limited identities and do not change atom positions in the laboratory.

Considering allowed variable ranges, we note that: (i) to preserve $0 \leq \alpha \leq \pi$, Eqs. (23a) and (23b) can only be used when $0 \leq \alpha \leq \pi/2$ and $\pi/2 \leq \alpha \leq \pi$, respectively, but (ii) to preserve $\beta_1 \geq 0$, these equations can only be used when $\beta_1 = 0$, i.e., can only be used on the $\beta_1 = 0$ boundary face. It is useful to treat Eqs. (23a) and (23b) as formal definitions of Ψ in the region where $\beta_1 < 0$. We then find from Eqs. (23c) and (23d), by canceling $|K_a, J, M\rangle e^{+im\alpha}$ (which is not zero everywhere) from both sides of the equation, that

$$(+i)^{m-K_a} f(-\beta_1, \beta_2) = +f(\beta_1, \beta_2), \quad (24a)$$

$$(-i)^{m-K_a} f(-\beta_1, \beta_2) = +f(\beta_1, \beta_2), \quad (24b)$$

for $0 \leq \alpha \leq \pi/2$ and $\pi/2 \leq \alpha \leq \pi$, respectively. Since $m - K_a$ must be even, Eqs. (24a) and (24b) both reduce to

$$(-1)^{(m-K_a)/2} f(-\beta_1, \beta_2) = +f(\beta_1, \beta_2), \quad (25)$$

for all $0 \leq \alpha \leq \pi$. Thus, when $m - K_a = 0$ or $2 \pmod 4$, $f(\beta_1, \beta_2)$ is an even or odd function of β_1 , respectively. Similar considerations, using abc and $abcd$ from Table 9 of [1], lead to

$$(-1)^{(m+K_a)/2} f(\beta_1, -\beta_2) = +f(\beta_1, \beta_2), \quad (26)$$

indicating that when $m + K_a = 0$ or $2 \pmod 4$, $f(\beta_1, \beta_2)$ is an even or odd function of β_2 , respectively. The requirements in Eqs. (25) and (26) on the even (e) or odd (o) behavior of $f(\beta_1, \beta_2) = f(ee), f(oo)$, etc. as a function of m and K_a are summarized in Table 4. This even or odd behavior gives the boundary conditions that must be applied at the $\beta_1 = 0$ (bottom) and $\beta_2 = 0$ (right) boundary faces, and requires in turn that either $f(\beta_1, \beta_2)$ or its derivative across the boundary must vanish at the boundary, e.g., for an $f(\beta_1, \beta_2)$ of the form $f(eo)$, we have $f(\beta_1, \beta_2) \neq 0$, but $\partial f(\beta_1, \beta_2)/\partial \beta_1 = 0$ at $\beta_1 = 0$, whereas $f(\beta_1, \beta_2) = 0$, but $\partial f(\beta_1, \beta_2)/\partial \beta_2 \neq 0$ at $\beta_2 = 0$.

Table 4

Symmetry properties^a of $f(\beta_1, \beta_2)$ as a function of the torsional and rotational quantum numbers^b m and K_a in basis functions of the form $|K_a, J, M\rangle e^{+im\alpha} f(\beta_1, \beta_2)$.

m	$K_a = 0^b$	1	2	3
0^b	ee^a	none ^c	oo	none
1	none	eo	none	oe
2	oo	none	ee	none
3	none	oe	none	eo

^a Symmetry properties indicated in this table by e (ven) and o (dd) are changes in sign of $f(\beta_1, \beta_2)$ with respect to a change in sign of either β_1 or β_2 , e.g., $f(eo)$ is unchanged when $\beta_1 \rightarrow -\beta_1$, but goes into its negative when $\beta_2 \rightarrow -\beta_2$. Even symmetry behavior near $\beta = 0$ can be represented by a power series in even powers of β (including a constant term); odd symmetry behavior leads to a series expansion in odd powers of β .

^b The quantum numbers m (left column) and K_a (top row) are both given *modulo* 4, so only four values are needed.

^c The entry “none” indicates that these combinations of m and K_a are not possible in the basis functions for this problem.

7.3. Boundary conditions for use with the single-valued coordinates in Fig. 2c–f

We do not investigate these four cases in detail here. We simply note that we can require that $\Psi \rightarrow 0$ as it approaches any of the faces on which $V = \infty$, but that determining the form of the boundary conditions on faces where V remains finite requires more work.

8. Comparison of the boundary conditions obtained in Section 7.2 for the single-valued coordinates in Fig. 2b with those obtained in [1] using extended PI group considerations

It can be shown as follows that the $G_4^{(8)}$ extended PI group treatment in [1], which uses an octuple-valued coordinate system, gives the same restrictions on m , K_a , and the boundary conditions for $f(\beta_1, \beta_2)$ as were obtained in Section 7.2. Table 5 gives $G_4^{(8)}$ species for the torsional (${}^t\Gamma$) and rotational (${}^r\Gamma$) basis functions, taken from Table 4 of [8], as well as species ${}^b\Gamma$ for the $f(\beta_1, \beta_2)$ bending functions appearing in Table 4 here. Table 6 gives the $G_4^{(8)}$ torsion-rotation species ${}^{tr}\Gamma$ for products of the torsional and rotational basis functions as a function of m and $K_a \bmod 4$.

The complete torsion-bending-rotational functions must belong to a species ${}^{tbr}\Gamma$ contained in the set of four single-valued representations of $G_4^{(8)}$ [1], namely $A_{1g}^+ \oplus A_{2g}^- \oplus B_{1u}^- \oplus B_{2u}^+$. Table 7 gives the types of functions $f(\beta_1, \beta_2) \pm f(\beta_2, \beta_1)$ that are compatible with this requirement, again as a function of m and $K_a \bmod 4$. (Note that these sum and difference bending functions belong individually to a nondegenerate species of $G_4^{(8)}$ if they are *ee* or *oo*, as defined in Table 7, but they belong as a pair to a doubly degenerate species if they are *eo* or *oe*.) Table 7 is the analog of Table 4, and the same rules are found in both tables, showing that the results from the treatment in [1] using an octuple-valued coordinate system are the same as those obtained in Section 7.2 using a single-valued coordinate system.

We note in passing that torsional and bending basis functions can each belong to one of only two different symmetry species in the PI group G_4 discussed in Section 6.2, whereas they each have five possible symmetry species in the octuple-group of [1].

9. Discussion

The use of methods based on multiple-valued coordinate systems (with the attendant creation of extra “non-physical” minima in the potential surface) versus the use of methods based on single-valued coordinate systems for treating the symmetry properties, energy levels, and wavefunctions of molecules with large-amplitude motions leads immediately to two questions. (i) Do calculations using these two methods give the same answers? (ii) If the answer to the first question is yes, then how are the mathematical constructs that exist in one method but not in the other related to each other? In this paper we have not investigated these questions in their full generality, but have instead considered only one

Table 5
Symmetry species in $G_4^{(8)}$ of the rotational (${}^r\Gamma$), torsional (${}^t\Gamma$), and bending (${}^b\Gamma$) factors in basis functions of the form $|K_a, J, M\rangle e^{i(m\alpha + J\beta_1 + \beta_2)}$.

m^a	${}^t\Gamma$	K_a^a	${}^r\Gamma$	$f(\beta_1, \beta_2)^b$	${}^b\Gamma$
0	$A_{1g}^+ \oplus B_{1u}^-$	0	$A_{1g}^+ \oplus A_{2g}^-$	<i>ee</i>	$A_{1g}^+ \oplus B_{2u}^+$
± 1	E_1	± 1	E_g	<i>eo</i> or <i>oe</i>	E^*
2	$A_{1u}^- \oplus B_{1g}^+$	2	$B_{1g}^+ \oplus B_{2g}^-$	<i>oo</i>	$A_{2u}^+ \oplus B_{1g}^+$

^a The quantum numbers in the m and K_a columns are given *modulo 4*.

^b $f(\beta_1, \beta_2)$ in this heading represents the pair of functions $f(\beta_1, \beta_2)$ and $f(\beta_2, \beta_1)$. The *ee*, *eo*, *oe*, and *oo* symbols are defined for each pair such that, for example, $f(eo)$ is unchanged (or multiplied by -1) if the variable in the first (or second) position is replaced by its negative.

Table 6

Symmetry species (${}^{tr}\Gamma = {}^t\Gamma \otimes {}^r\Gamma$) in $G_4^{(8)}$ of the torsion-rotation product basis functions $|K_a, J, M\rangle e^{i(m\alpha)}$ in Table 4.

m^a	$K_a^a = 0$	± 1	2
0	$A_{1g}^+ \oplus A_{2g}^- \oplus B_{1u}^- \oplus B_{2u}^+$	$E_g \oplus E_u$	$A_{1u}^- \oplus A_{2u}^+ \oplus B_{1g}^+ \oplus B_{2g}^-$
± 1	$E_1 \oplus E_2$	$E^* \oplus E^-$	$E_1 \oplus E_2$
2	$A_{1u}^- \oplus A_{2u}^+ \oplus B_{1g}^+ \oplus B_{2g}^-$	$E_g \oplus E_u$	$A_{1g}^+ \oplus A_{2g}^- \oplus B_{1u}^- \oplus B_{2u}^+$

^a The m and K_a quantum numbers are given *modulo 4*.

Table 7

Bending functions of the form $f(\beta_1, \beta_2) \pm f(\beta_2, \beta_1)$ that are compatible in $G_4^{(8)}$ with the m and K_a quantum numbers listed.

m^a	$K_a^a = 0$	± 1	2
0	<i>ee</i> ^b	<i>none</i> ^c	<i>oo</i>
± 1	<i>none</i>	<i>eo</i> or <i>oe</i>	<i>none</i>
2	<i>oo</i>	<i>none</i>	<i>ee</i>

^a The m and K_a quantum numbers are given *modulo 4*.

^b The first (or second) letter in the *ee*, *eo*, *oe*, and *oo* entries indicates (*e*)ven or (*o*)dd behavior of the function $f(\beta_f, \beta_s)$ when the first argument β_f (or the second argument β_s) is replaced by its negative.

^c The entry “none” indicates that no bending functions have suitable symmetry for these sets of m and K_a .

molecular example, i.e., the trans-bent and cis-bent minima on the S_1 electronic potential surface of acetylene, and only one class of molecule-fixed coordinates, i.e., coordinates describing center-of-mass translation, overall rotation, small-amplitude vibrations, and large-amplitude motions. Even for this relatively specialized single example, we have made no attempt to investigate question (i) with numerical calculations, but have instead focused on the algebra associated with question (ii).

This algebra suggests (at least to the author) that for this example, the same numerical results for energy levels and wavefunctions will be obtained from both methods. However, convincing empirical proof of this statement will in fact require carrying out at least two rather accurate numerical calculations for the same potential surface, one using multiple-valued coordinates, the other using single-valued coordinates. Even more convincing would be additional calculations using single-valued coordinate systems dramatically different from the type discussed here (e.g., Jacobi coordinates).

What the present work does establish, is that for the molecule-fixed coordinates discussed here, it is possible to move back and forth between multiple-valued and single-valued coordinate systems by suitably enlarging or restricting the range of appropriate LAM coordinates. When this is done, basis-set behavior that appears as a group-theoretical symmetry property under coordinate transformations in the larger coordinate range of the multiple-valued coordinate system, is changed into basis-set behavior on one of the boundaries of the smaller coordinate range of the single-valued coordinate system, i.e., appears as a basis set boundary condition on a boundary where the potential energy V remains finite. This can be made intuitively reasonable by noting, as was pointed out in Section 3.3, that the diagonal associated with PI-group symmetry behavior becomes the diagonal associated with boundary condition behavior, and vice versa, when one switches from a consideration of the upper left triangle in Fig. 1c to a consideration of the lower left triangle in Fig. 1d as the domain containing allowed values of the single-valued two-bending-angle coordinate system. Whether this conversion of the extended-group symmetry behavior of Ψ into differential-equation boundary-condition behavior of Ψ on boundary lines or surfaces where $V \neq \infty$ will apply to other, conceptually very different, types of molecule-fixed coordinates has not been investigated.

Another question that quickly comes to mind, is whether these same arguments can be applied to a bent triatomic molecule with a very large-amplitude bending vibration, i.e., to a quasilinear triatomic molecule. In the author's opinion, a bent triatomic molecule has an additional complication, which was avoided here because of the high barrier to linearity for bent acetylene in its S_1 state. In the present problem, the division into rotational and vibrational degrees of freedom is quite clear, i.e., there are three rotational degrees of freedom, characterized by three Eulerian angles and three finite rotational constants, and there are $3N - 6 = 6$ vibrational degrees of freedom, divided into small and large amplitude categories. For a linear triatomic molecule, which cannot undergo LAM bending without passing through the linear configuration, where A in the rotational operator AJ_z^2 becomes infinite, complications associated with this infinity must be properly dealt with. It would clearly be interesting to consider the bending motion of a triatomic molecule using multiple-valued coordinates to determine in detail exactly where in the mathematics, and how, the arguments used in [1] would break down.

Finally, a point of potential concern arises because the internal rotation angle α (i.e., the $H_1-C_a-C_b-H_2$ dihedral angle) is not defined in the half-linear transition state, but this problem appears to be an artifact of the angular coordinate system used to describe trajectories of the hydrogen atoms H_1 and H_2 on the spheres shown (as circles) in Fig. 3a of Ref. [1]. The local-mode bending trajectories for H_1 and H_2 correspond approximately to the circular arcs traced out by rotating the C_aH_1 and C_bH_2 bonds around axes passing through the C_a and C_b atoms, respectively, and directed parallel to the y axis. These motions must be coordinated so that the molecule never becomes linear. The internal rotation trajectories for H_1 and H_2 correspond approximately to the circles traced out by rotating the C_aH_1 and C_bH_2 bonds by equal amounts in opposite senses around the z axis.

It can be seen that the circular arcs and circles traced out by these bending and internal rotation trajectories do not intersect, except at their initial and final points. This is important because multi-dimensional high-barrier tunneling treatments will break

down if the part of the wave packet traveling along one tunneling path can communicate significantly with the part traveling along another tunneling path. Of course the question of whether these assumed tunneling paths are truly isolated from each other on the S_1 potential surface of acetylene must ultimately be answered by examining the agreement of theoretical predictions (e.g., K-staggering [1]) with experiment, or by examining the landscape of maxima, saddles, and minima on the S_1 potential surface produced by very accurate quantum chemical calculations.

It can be seen that these circular paths on the surface of the spheres in Fig. 3a of [1] are mathematically well-behaved everywhere, in the sense that they are continuous and have continuous derivatives with respect to distance along the path. This suggests that no mathematical difficulties will be encountered along these paths, in spite of the fact that the torsional angle is indeterminate at the midpoint of either bending trajectory (much as the longitude is indeterminate at the north and south poles of the earth, even though the poles themselves are no different than any other points on the earth's surface).

Acknowledgments

The author is greatly indebted to Dr. Tucker Carrington, Jr. for stimulating and provocative discussion of many of the topics in this paper, and to Drs. A.J. Merer and J.H. Baraban for helpful comments and criticisms of a draft of this manuscript.

References

- [1] J.T. Hougen, A.J. Merer, *J. Mol. Spectrosc.* 267 (2011) 200–221.
- [2] E. Ventura, M. Dallos, H. Lischka, *J. Chem. Phys.* 118 (2003) 1702–1713.
- [3] J.H. Baraban, A.R. Beck, A.H. Steeves, J.F. Stanton, R.W. Field, *J. Chem. Phys.* 134 (2011). 244311-1–244311-10.
- [4] J.F. Stanton, C.-M. Huang, P.G. Szalay, *J. Chem. Phys.* 101 (1994) 356–365.
- [5] J.T. Hougen, *J. Mol. Spectrosc.* 256 (2009) 170–185.
- [6] J.H. Baraban, private communication.
- [7] E.P. Wigner, *Group Theory*, Academic Press, 1959.
- [8] A.J. Merer, J.K.G. Watson, *J. Mol. Spectrosc.* 47 (1973) 499–514.